

1 **In-situ Decomposition Sensor Output Correlates with Soil**
2 **Health Indicators**

3 Taylor J. Sharpe¹, Madhur Atreya², Shangshi Liu^{3,1}, Mengyi Gong⁴, Nicole Luna², Noah Smock²,
4 Jessica Davies⁵, John N. Quinton⁵, Richard D. Bardgett³, Jason C. Neff⁶, Rebecca Killick⁴,
5 Gregory L. Whiting^{2,7,*}

6 ¹Mortenson Center in Global Engineering, University of Colorado Boulder, 4001 Discovery
7 Drive, 608 UCB, Boulder, CO 80303, USA

8 ²Paul M Rady Department of Mechanical Engineering, University of Colorado Boulder, 1111
9 Engineering Drive, UCB 427, Boulder, CO 80309, USA

10 ³Department of Earth and Environmental Sciences, The University of Manchester, Michael
11 Smith Building, Manchester M13 9TP, UK

12 ⁴School of Mathematical Sciences, Lancaster University, Flyde Ave, Bailrigg, Lancaster LA1
13 4YR, UK

14 ⁵Lancaster Environment Centre, Lancaster University, Library Ave, Bailrigg, Lancaster LA1
15 4YQ, UK

16 ⁶Environmental Studies, University of Colorado Boulder, 4001 Discovery Drive, 397 UCB,
17 Boulder, CO 80303, USA

18 ⁷Materials Science and Engineering Program, University of Colorado Boulder, 4001 Discovery
19 Drive, 613 UCB, Boulder, CO 80303, USA

20 ¹Current address: Yale Center for Natural Carbon Capture, Yale University, PO Box 208109,
21 New Haven, CT 06520, USA

22 *Correspondence to: gregory.whiting@colorado.edu

23

24 **Abstract**

25 Monitoring of soil microbiological processes can inform strategies to improve soil health and
26 agricultural productivity. Biological soil health measurements are currently difficult to make in-
27 situ and in real time, usually involving manual sampling and laboratory analysis. This is costly,
28 time consuming, resource intensive, and cannot measure changes at high temporal and spatial
29 resolution, limiting the ability to make prompt informed land management decisions. Low-cost
30 soil sensors manufactured using printing techniques offer a potential scalable solution to these
31 issues. Here, we tested the use of novel sensors for the proxy evaluation of soil microbial
32 processes, hypothesizing that sensor decomposition rates may be related to manual soil sampling
33 measurements. This is the first multi-plot field deployment of sensors which use a biodegradable
34 composite conductor to transduce microbial decomposition of substrates to a change in electrical
35 resistance, providing time-series decomposition rate data. Sensors were installed for 50 days
36 across 44 experimental plots of a long-term grassland experiment with varying historical
37 treatments and significant differences in soil microbial activity. Early failures and unresponsive
38 substrates reduced the included sensor count to 31. Measurements commonly used as soil health
39 indicators, including microbial biomass and enzymatic activities related to nutrient cycling, were
40 determined using standard laboratory methods and compared to sensor responses. Three
41 statistical approaches found positive correlations between the sensor signal and laboratory
42 measurements of microbial biomass carbon and soil organic carbon, and some approaches found
43 weaker correlations with enzymatic measurements. Although this experiment is limited in scope
44 to a single experimental field and season, these initial findings show promise for enabling the
45 proxy measurement of soil microbial processes in-situ using low-cost, scalable printed sensors.

46 **Keywords**

47 Printed Electronics, In-situ Sensing, Soil Biological Activity, Soil Health, Soil Sensing

48

49 **1. Introduction**

50 High spatial and temporal resolution monitoring of soils is required to accurately manage soil
51 resources [1], but currently we have limited capability beyond the monitoring of soil water,
52 temperature, and some chemical parameters.

53 Soil health refers to a broad set of metrics and methodologies that relate to a soil's ability to
54 provide ecosystem services [2]. Soil health indicators are usually broken into three categories:
55 physical, chemical, and biological [3,4], with biological indicators receiving relatively less
56 attention in soil health assessments [5,6]. This is due in part to difficulties in both the
57 measurement and integration of biological parameters into soil health models [7]. There is broad
58 agreement that more comprehensive soil health models would place greater weight on biological
59 measurements [8,9]. Conventional laboratory methods for assessing soil biological properties
60 that are key to soil health (Table 1) are typically carried out on samples taken from the field and
61 analyzed in the laboratory. This means that the conditions of the sample may no longer reflect
62 those in the field. Additionally, lab analyses can be expensive and time consuming, do not
63 provide the benefits of continuous, in-situ monitoring [10], and in the case of microbial biomass
64 carbon (MBC) and genetic sequencing, do not differentiate between currently active microbes
65 and relic materials from the microbial necromass [11]. Techniques involving the burial of
66 organic matter such as litter bags, wood, cotton strips, or tea bags, are advantageous due to their
67 simplicity and the fact that they represent the rate of organic matter decomposition in-situ [12].
68 However, they require retrieval, drying, and weighing, limiting their utility at identifying short-
69 term changes in decomposition rates or critical change points. Similarly, nitrogen mineralization
70 techniques can capture in-situ effects with the use of soil buried in gas permeable containers
71 [13], but require retrieval and laboratory analysis. As such, there is a need for better ways to
72 evaluate the biological components of soil health at scale, including the implementation of
73 continuous monitoring to evaluate changing trajectories.

74

75

76

77

78

79

80

81

82 Table 1: Comparison of methods commonly used for determining microbial activity in soils.

	PHBV:C Decomp. Sensor (this work)	Litter Bag / Wood / Standard Decomp. [12,14,15]	CO₂ Chamber Methods [16]	Nitrogen Mineraliz- ation [13,17]	MBC Lab Test [18]	Enzyme Activity [19]	PLFA Lab Test [20]	Genetic Sequencing [21,22]
<i>In-Situ?</i>	Yes	Yes / episodic	Yes / episodic	Yes	No	No	No	No
<i>Continuous Signal?</i>	Yes	No	Yes	No	No	No	No	No
<i>Sensed property</i>	Substrate -specific decompo- -sition	Mass change of organic matter	Soil respiration (plant and microbial)	Rate of Nitrogen species conversion	Total microbial biomass	Enzymatic functional	Fatty acid across taxa	Broad microbial composition
<i>Living organisms only?</i>	Yes	Yes	Yes	Yes	No	Yes	Yes	No
<i>Time Integration</i>	Long- term time series	Long-term time series	Short-term time series	Snapshot / Short-term time series	Snapshot	Snapshot	Snapshot	Snapshot
<i>Relative Sample Costs</i>	\$	\$	\$\$\$\$	\$\$	\$\$	\$\$	\$\$	\$\$\$

83
84 Continuous monitoring of soil microbiological activity has been primarily restricted to
85 measuring soil CO₂ fluxes [23], manual measurement of tea bag, cotton, or wood decomposition
86 during burial [12], controlled laboratory analysis, or small-scale applications of prototype
87 sensors [24]. Fine-scale CO₂ flux measurements rely on either regular visits to the field to take
88 gas samples from chambers or the use of expensive automated chamber systems; neither can
89 differentiate root and soil respiration or provide truly continuous measurements. Real-time
90 monitoring of soil biological activity would enable precise and sustainable management of this
91 key component of soil. This is particularly important given the fundamental importance of the
92 soil microbiome for maintaining soil health and ecosystem functioning [25,26]. These critical
93 soil functions include nutrient cycling, decomposition, plant growth, and mediation of soil
94 carbon fluxes due to respiration and sequestration [27–29]. Microorganisms in the soil affect the
95 fate and transport of carbon in the largest terrestrial carbon pool on the planet [30]. In addition,
96 they contribute to critical ecosystem services from the provisioning of food and safe drinking
97 water to the regulation of pathogenic organisms [31].

98 Emerging technologies have shown promise in supporting programs to restore soil health,
99 including remote sensing, mobile applications, and in-situ sensors [32]. However, monitoring
100 systems have challenges to overcome, including energy efficiency constraints, cost, response
101 time, accuracy, and ease of use [33]. Due to their heterogeneity, soils can be particularly hard to
102 meaningfully monitor without high spatial coverage, with soil microbial communities and soil
103 properties showing high spatial and temporal variability [11,34]. Print-based fabrication of
104 electronic devices offers a potential solution to several of these limitations, as the low cost of
105 manufacturing allows for large-scale deployment with high sensor counts, enabling high spatial
106 and temporal resolution for soil monitoring. Others have demonstrated the utility of a variety of
107 printed electronic sensors applied in the continuous monitoring of soil physical and chemical
108 properties, including moisture [35–37], relative humidity [38], pH [39–41], nitrate [42–45], and
109 chloride [46,47]. We have previously demonstrated printed electronic sensors which transduce
110 microbial decomposition activity into electrical resistance changes as soil microbes degrade a
111 poly(hydroxybutyrate-co-valerate) (PHBV)/carbon composite conductor [24]. In this approach,
112 the PHBV biopolymer (which is degraded in both aerobic and anaerobic conditions [48]), is
113 blended with carbon flake to form a printable ink. Using a stencil-printing process, the ink is
114 deposited onto a surface and dried to create a resistor which is responsive to microbial activity.
115 As the resistor is decomposed in the soil, it swells more effectively, leading to an increase in
116 resistance over time with a gradient which dynamically corresponds to the level of microbial
117 activity. Controlled experiments comparing sensor response in active and sterilized compost tea
118 showed a sensor response only in the non-sterile case. In relatively sterile environments, such as
119 autoclaved sand or deionized water, the resistor showed a negligible change in resistance over
120 time, further suggesting microbial activity as the primary contributor to sensor response. The
121 resistance changes that are provided by the sensor are trivially simple to measure using
122 conventional low-cost electronics, thereby supporting high-density deployments that can help
123 keep instrumentation costs low.

124 The goal of this work was to determine whether PHBV/carbon decomposition sensor signals
125 mirrored more conventional measurements from various soil plots. Here, the performance of and
126 methods for use and analysis of these sensors is evaluated in a first multi-plot field deployment
127 within a long-term grassland biodiversity restoration experiment in northern England. This site
128 includes experimental treatments of different agricultural management practices, which have led
129 to significant differences in soil properties and plant productivity over the site. We compared
130 signals from the sensors and related them to standard measures of soil microbial biomass and
131 function across 44 experimental plots over 50 days during the summer of 2023. Previous studies
132 at this deployment site have demonstrated significant shifts in microbial communities, including
133 their biomass and activity in response to management treatments [49]. As such, this experiment
134 provided an excellent basis for examining the function of these novel sensors and the relationship
135 between their response and traditional laboratory soil measurements.

136 This new sensing modality provides real-time information about rates of decomposition of a
137 biodegradable substrate. This process is downstream of various drivers of decomposition in soils,
138 including soil temperature, moisture and pH. Rather than considering these confounders
139 separately, these sensors directly measure substrate decomposition. We hypothesized that these
140 decomposition sensors could correlate to soil health-related laboratory measurements within the
141 scope of this study, enabling useful proxy soil biological measurements in the case of a single
142 historical field site. Successful correlation to existing biological soil health indicators would
143 suggest possible future utility of the technology.

144 **2. Materials and Methods**

145 **2.1. Sensor Fabrication**

146 The deployed sensors were prepared according to previous reports [24]. A single loop microbe
147 responsive resistor (width 3 mm, length 75 mm) composed of a PHBV/carbon flake composite
148 was printed using a laser-cut tape stencil on to a glass substrate. A conductive epoxy (*MG*
149 *Chemicals 8331D*) was used to connect two leads at either side of the trace, followed by dipping
150 in a weatherizing adhesive (*FlexSeal*) to waterproof the connections. This left a large portion
151 conductive polymer trace exposed (Figure 1b). Roughly 60mm of trace is left exposed following
152 the epoxy process, resulting in a sensing area of roughly 33mm². Each sensor has a waterproof
153 connector at the end of a signal wire. 82 sensors were initially fabricated with an average
154 resistance of 2.88 k Ω \pm 0.43 k Ω (standard deviation). Seven outliers were removed to yield a
155 final average sensor resistance of 2.95 k Ω \pm 0.22 k Ω .

156 Sensor readout was achieved using custom made data loggers, where each logger supports up to
157 six channels through which individual sensors can be read. Loggers were produced using low-cost
158 electronics, including an SD-card enabled microcontroller (*Arduino, Inc.*), a lithium polymer
159 battery, a watertight enclosure, and a timing circuit which provided power to the microcontroller
160 every 30 minutes.

161 **2.2. Experimental Site**

162 The study took place in Colt Park Meadows, located in the Ingleborough National Nature
163 Reserve (Latitude 54°12'N, Longitude 2°21'W, 350 m.a.s.l.) in the United Kingdom. The test
164 site is part of a long-term grassland biodiversity restoration experiment established in 1989 on
165 agriculturally improved, species-poor mesotrophic grasslands [50]. It has provided a variety of
166 management-relevant experimental restoration treatments on a field scale. The soil at this site is
167 a moderate to high residual fertility clayey Brown Earth over limestone bedrock (clay + silt \approx
168 60–70%), belonging to the Malham series of Eutric Endoleptic Cambisols, with an average soil
169 organic carbon content of about 8.3% and a pH of \sim 5.8 [51,52]. These grasslands have been
170 targeted by various environmental land management schemes aimed at enhancing botanical
171 diversity and soil health [53,54]. The experiment includes four main treatments with their

198 **Figure 1.** (a) Diagram showing the placement of printed decomposition sensors and loggers in
199 the field, including sensing surface depths. (b) Image of a single decomposition sensor as
200 fabricated for this field deployment.

201 The state of the sensors was continuously monitored over the course of 50 days using custom
202 waterproof data loggers each capable of interrogating up to 6 individual sensors through wired
203 connections, as depicted in Figure 1. As Colt Park is located in a field at some distance from
204 reliable internet connection, data loggers collected data via SD card rather than using WiFi or
205 other telemetry options.

206 **2.4. Lab Analysis**

207 Within each plot, soil sampling methods were used to obtain laboratory measurements for a
208 variety of chemical and biological parameters near the mid-point of the deployment period, in
209 mid-July. At least three soil cores were collected approximately 30 cm from the sensors. This
210 proximity was selected to balance two factors: it is sufficiently close to ensure that laboratory
211 soil health indicators remain spatially representative of the sensor data, yet distant enough to
212 prevent sampling-induced disturbances, such as altered water infiltration or oxygen diffusion
213 caused by macropores, from potentially interfering with the sensor readings. The cores from each
214 plot were then composited prior to laboratory analysis.

215 Lab measurements included soil organic content (SOC), determined by an elemental analyzer
216 (Elementar Vario EL CN analyzer) as no detectable inorganic carbon was found in the samples.
217 Additionally, three extracellular enzyme activities were measured by standard colorimetric
218 analysis [59]: glucosidase (GLC), glucosaminidase (NAG), and phosphatase (PHO), which
219 represent carbon, nitrogen, and phosphorus decomposition or acquisition enzymes, respectively.
220 Microbial biomass carbon (MBC) was obtained using the fumigation-extraction method [60].

221 **2.5. QC and Filtering**

222 The soil decomposition sensors generally show an increasing resistance over time in response to
223 microbial activity in the soil (Supplemental Figures S1, S2). Resistances are normalized by
224 dividing all readings by the initial resistance of each sensor (Supplemental Figure S3). At some
225 point – typically weeks after installation for this materials set and sensor design – the resistor
226 material is sufficiently damaged by microbial activity and the resistance rapidly increases
227 indicating that the device has reached the end of its useful lifetime. After an initial settling time
228 and prior to this failure point, the sensor signal defines a decomposition window in which useful
229 data can be extracted. In some cases, likely due to variability related to the fabrication process or
230 issues which occur during installation, a sensor will either be non-responsive or will fail very
231 rapidly in comparison to other devices. These devices are identified through data filtering. Our
232 first step in the data analysis pipeline was to use a polynomial fitting algorithm to remove these
233 anomalous signals. Devices with a low correlation coefficient ($R^2 < 0.5$) from a second-order

234 polynomial regression were removed from the analysis, along with two additional sensors which
 235 had spuriously high initial resistance, likely caused by trace damage on soil insertion
 236 (Supplementary Figure S2). This filtering approach shows sensitivity to the selection of the pre-
 237 analysis filter threshold (Supplementary Table S6). We chose the 0.5 R^2 threshold because the
 238 results most closely aligned with our visual examination of sensor signals, and this threshold
 239 maintained just over 70% of the installed sensors. The 0.5 R^2 threshold left 31 sensors for
 240 inclusion in the analysis. Totals for each sensor category are shown in Table 2 below.

241 Table 2: Sensor counts included and removed from the analysis, with failure modes identified.

	Included	Removed (Rapid Response)	Removed (No Response)	Removed (Trace Damaged)
Sensor n	31	5	2	6
Sensor %	70.5%	11.4%	4.5%	13.6%
Total by Category	31 / 70.5%	Removed: 13 / 29.5%		

242

243 2.6. Statistical Approaches

244 To understand how various analytical approaches impact correlation to other field measurements
 245 within the remaining data set, three analyses (Figure 2) were then evaluated: a global
 246 decomposition window approach (Analysis 1), an individual sensor approach with two varying
 247 decomposition phases (Analysis 2), and a sensor signal changepoint count analysis (Analysis 3).
 248 In all analysis approaches described here, a single time-integrated measurement results from
 249 processing time series data, either by taking the slope of the sensor's normalized resistance or by
 250 counting the number of changepoints detected in the signal. In other words, all analyses depend
 251 on a structured dataset in which the base sampling unit is the soil plot; for each plot, a single
 252 slope or changepoint count total is compared to mid-experiment traditional laboratory
 253 measurement. The correlations between the time-integrated measurements and the laboratory
 254 measurements are then investigated to establish the connection between sensor signals and soil
 255 microbial activities.

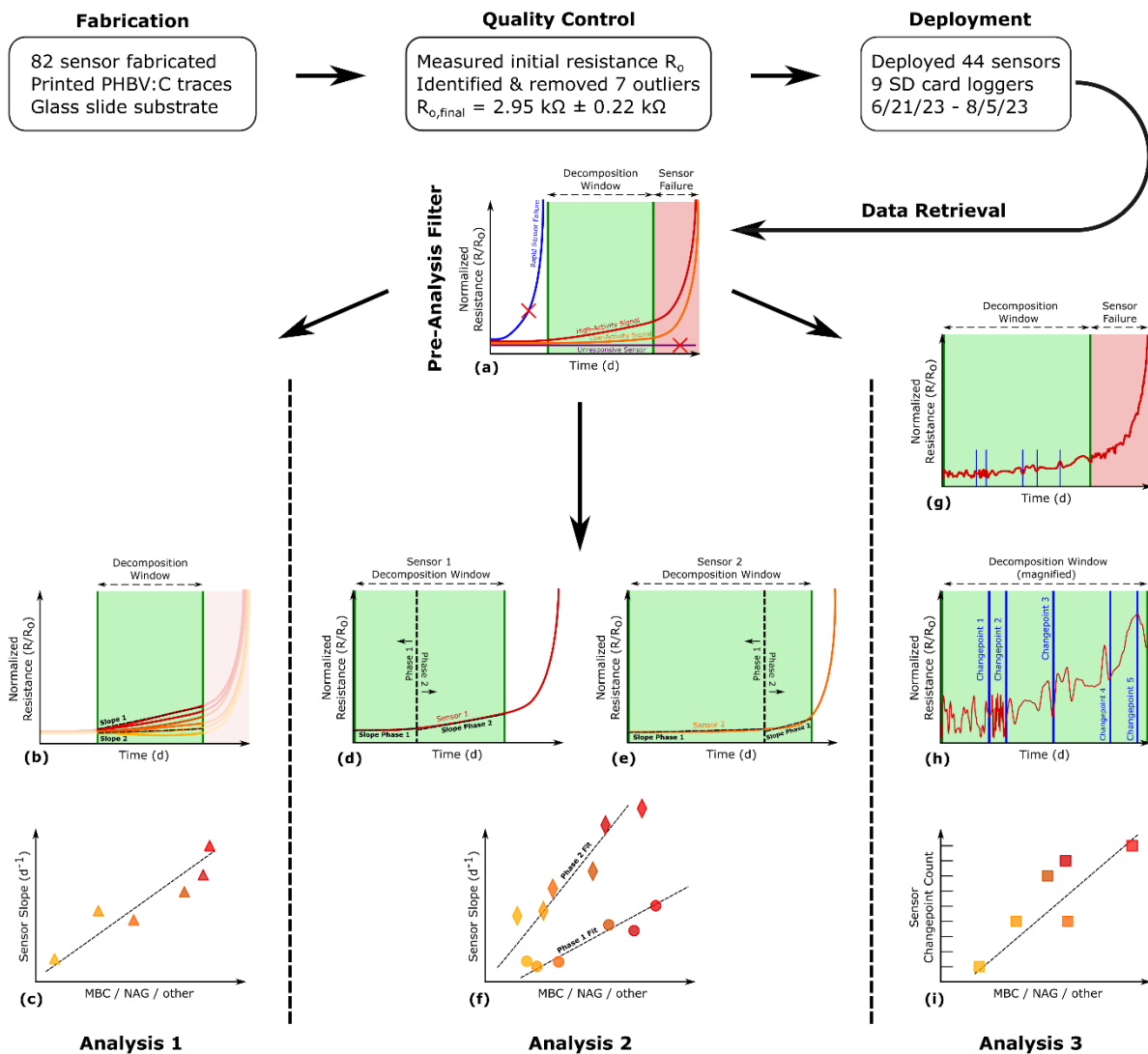
256 Analysis 1 evaluated all 31 sensor responses using a single decomposition window. To define a
 257 decomposition window for analysis, all filtered sensor signals were averaged, and changepoint
 258 detection was used to define the point at which the average sensor signal changes significantly
 259 (Supplemental Figure S4). In this case, changepoint detection was performed by looking for the
 260 location of change in variance in the first-order difference time series using the Binary
 261 Segmentation method with a maximum of 3 changepoints. This defined the end of the
 262 decomposition window and the beginning of the sensor failure phase. The signal following this

263 sensor failure time was removed from the dataset. Next, the same changepoint detection
264 algorithm was applied to the remaining data to define the beginning of the decomposition
265 window following sensor settling in the soil. A short buffer of three days was applied at the
266 beginning and end of the window to isolate the region in which sensor responses are well-
267 defined (Supplemental Figure S5). Each sensor's slope within the decomposition window was
268 calculated using a second-order polynomial regression, and we took the linear coefficient to be
269 the slope. On a per-sensor basis, sensor slopes were then calculated and compared to laboratory
270 measurements within the plots.

271 Analysis 2 differs from Analysis 1 in two primary ways: first, we considered individual
272 decomposition windows on a per-sensor basis, varying the beginning and end of the period
273 included in the analysis by sensor signal. Second, visual examination of the sensor signals
274 suggested two distinct phases of decomposition, with the slope increasing more rapidly in a
275 phase prior to total sensor failure, so we aimed to investigate the relationship between the rate of
276 decomposition and the soil parameter measurements in two phases. In this analysis, two
277 changepoint analyses were applied to each individual sensor signal iteratively. First, the pruned
278 exact linear time (PELT) method with manually selected penalty [61] was applied to each
279 individual sensor signal to identify changes in variance in the first-order difference time series.
280 The time of failure is defined as the changepoint where the ratio of variance before and after the
281 changepoint reaches the maximum. A minimum decomposing time of 10 days was used to avoid
282 the identification of unrealistic early time of failure due to the division of a moderate variance by
283 a very small variance in the segment before the changepoint. The signal beyond this point was
284 removed from the analysis. A second changepoint detection, assuming there is at most one
285 change (AMOC, estimated using likelihood ratio test-based method) in the slope of the linear
286 regression model, was then used to differentiate phase 1 and phase 2 within the remaining
287 decomposition signal. Finally, a linear regression model was applied to each phase. The
288 estimated slope parameters from the two phases were correlated to soil parameter measurements
289 respectively (Supplementary Figure S6).

290 Analysis 3 focused on the number of significant changepoints observed in a given sensor's
291 signal, rather than the rate of sensor decomposition. This analysis does not require the definition
292 of any specific decomposition window, looking instead at the total number of changepoints
293 detected in a particular sensor's signal during deployment prior to sensor failure. For this
294 approach the failure time of each sensor signal is detected in the same way as described for
295 Analysis 2. Whereas the previous two analyses considered a polynomial or linear regression
296 model for the data within the decomposition windows, we instead continued with the
297 changepoint approach and allowed the number of changepoints to be estimated (Supplementary
298 Figure S7). The changepoint model finds structural breaks in the decomposition time series due
299 to changes in linear and/or quadratic trend to model more local features and is fitted using the
300 optimal pruned exact linear time (PELT) changepoint search algorithm [50], with manually
301 selected penalty. The number of detected changes was then correlated to soil parameter

302 measurements (Figure 2, Analysis 3). A table summarizing the statistical methods used in the
 303 three analyses and the derived metrics is given in supplemental Table S3.



304 **Figure 2.** Illustration of the data pipeline for the three analysis approaches. Following
 305 fabrication, deployment, and data retrieval, stochastic sensor signals were removed by the pre-
 306 analysis filter prior to all correlation analyses (a). For Analysis 1, slopes within the
 307 decomposition window were extracted and correlated to laboratory measurements (b, c).
 308 Analysis 2 broke each sensor signal into two sensor-specific decomposition windows (d, e). On a
 309 per-sensor basis, correlations were then taken between the measured parameter and slopes within
 310 each phase (f). Analysis 3 used the number of decomposition function changepoints as a proxy
 311 for microbial activity and stability, breaking each sensor signal into sensible changepoints (g, h).
 312 On a per-sensor basis, the number of changepoints was then correlated to each measured
 313 parameter (i).
 314

315 To determine whether the sensor signal mirrored biogeochemical differences in instrumented
316 plots, we carried out a series of regression analyses of sensor signals against measured soil
317 attributes and present these analyses with estimated correlation coefficients and p values. Tests
318 of the validity of model assumptions are presented in Supplemental Table S2. It should be noted
319 that based on the focus of the study, sufficient sensors were not available to replicate a standard
320 randomized design for evaluation of treatment differences, but we have visualized treatment
321 effects over our primary findings (Supplementary Figure S14). The statistics extracted from the
322 regression and changepoint analyses are time-integrated measures which are hypothesized to
323 reflect the level of soil microbial activities during the monitoring window. The soil microbial
324 parameters obtained from the fieldwork, despite being one-off measurements, are expected to be
325 stable over the monitoring period [62]. Here we investigated the relationship between these
326 measurements and the extracted statistics to gain insight into the sensor responses to soil
327 microbial activities.

328 All data analysis was carried out with R version 4.3.2. utilizing R packages changepoint for
329 implementing the binary segmentation and the PELT methods for identifying changes in
330 variance and R package EnvCpt for detecting changes in trend in the linear or polynomial
331 regression models [63,64]. The tests on regression model assumptions were carried out using the
332 R package lmtest [65].

333 **2.7 Interference Experiments**

334 Because this experiment did not include the co-deployment of traditional in-situ sensors in each
335 soil plot, ambiguity exists in the signal. Resistance changes in the sensor substrate can be the
336 result of abiotic processes including changes in soil moisture and temperature. Rainfall and air
337 temperature data from a nearby weather station (Ribblehead Station, ~1.7 km from Colt Park
338 [66]) were collected and visualized alongside minimum, maximum, and median sensor signals in
339 supplementary figure S15.

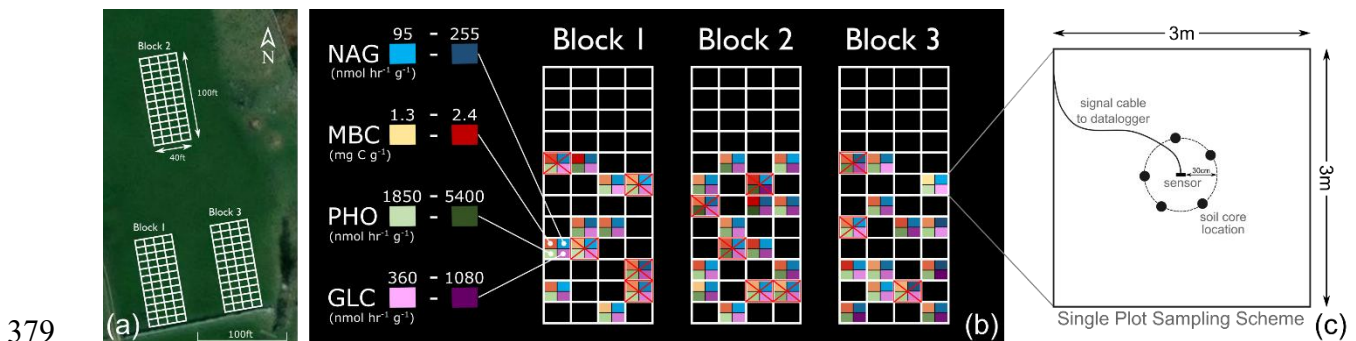
340 To more fully characterize the impacts of local soil conditions, we conducted a set of
341 interference experiments over short time periods to isolate impacts on the signal from microbial
342 decomposition. New sensors were produced and installed in soil in the lab. Varying one
343 parameter at a time, continuous resistance outputs were collected. Temperature was varied by
344 installing the soil sample in a heating coil within a refrigerator; a temperature controller swept
345 across a range from 5.4 to 23.5 °C. Volumetric water content was varied from 18.9% to 46.4%,
346 and soil conductivity was modified by alternating between DI water and dissolved NaCl
347 application, giving a range from 437 to 1120 $\mu\text{S}/\text{cm}$. Soil moisture, temperature, and
348 conductivity were measured simultaneously using a TDR-310H (Acclima) with data collected
349 with a DataSnap logger (Acclima). Readings were collected every 5 minutes.

350 **3. Results and Discussion**

351 **3.1. Soil indicators**

352 As expected, due to differing soil conditions originating from combinations of historical
353 management treatments, lab measurements of soil parameters show a wide range of values across
354 the experimental plots. These indicators are used in current soil health measurements [5,67–69],
355 and are commonly known as key factors controlling soil organic matter decomposition rates.
356 SOC is one of the most widely used soil health indicators [5], given its role in enhancing soil
357 physical stability, improving water retention, and carbon sequestration. The SOC content ranges
358 from 6.65% to 10.58% across all plots, indicating generally high but variable substrate
359 availability for microbial decomposition. MBC represents a small yet active carbon pool in this
360 study, comprising approximately 2.1% of the total SOC on average, consistent with findings
361 from other studies [70]. It has been suggested as dominant factor that controls the overall
362 decomposition rate of soil organic matter [71]. Microbial biomass is considered a conservative
363 indicator of soil biological status, showing lower short-term variability than more labile
364 indicators, such as extracellular enzymes [72]. Similarly, SOC is well-established as a slowly
365 changing pool, typically requiring years to decades of altered management to detect significant
366 changes [62]. Although MBC tends to show higher temporal dynamics than SOC, there was no
367 significant environmental perturbation during the sampling period, and evidence indicates that C-
368 rich and low-pH soils, such as the ones at our study site, tend to dampen the temporal variability
369 of microbial biomass [73].

370 Extracellular enzymes in the soil, mainly produced by microbes, are directly involved in the
371 breakdown of certain organic materials and nutrient cycling (e.g., carbon, nitrogen, phosphorus
372 cycling), thereby directly affecting plant growth and soil fertility [74], and can be used to
373 indicate substrate-specific decomposition processes. The enzymes measured here also exhibit
374 high spatial variability (Figure 3), highlighting their sensitivity to management differences.
375 Monitoring these parameters helps in understanding the impacts of ecosystem management
376 practices and environmental changes on soil health and guides sustainable soil management
377 strategies. For the purposes of this study, these measurements demonstrate that a wide range of
378 soil conditions exist at this test site (Supplementary Figure S16).

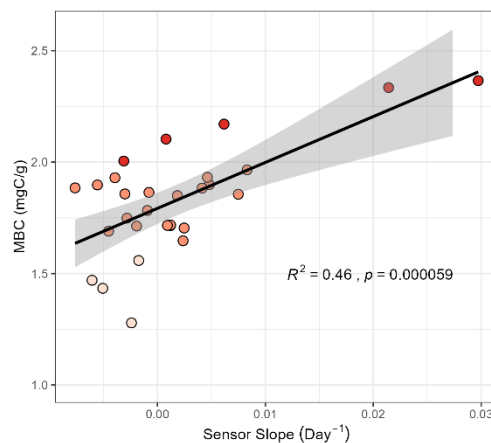


380 **Figure 3.** (a) Satellite image of Colt Park Meadows, showing the positions of the 3 replicate
381 experimental blocks, each of which contain 48 plots (*EarthSat image courtesy of the U.S.*
382 *Geological Survey*). (b) Colors show relative results from biological soil enzyme measurements
383 taken from within instrumented plots. Sites where sensors failure led to removal from the final
384 analysis are indicated with red X icons. (c) At each plot, the sensor was installed at the middle of
385 the plot, and soil samples were taken at a distance of ~30cm from the sensor.

386 3.2. Sensor Data Analysis

387 3.2.1 Analysis 1: Global Decomposition Window

388 The results of Analysis 1 indicate that the rate of resistance change recorded by the sensor is
389 correlated with conventional measures of microbial biomass and activity, with significant
390 variability due to the hardware constraints of the deployed sensors. A positive correlation was
391 observed with MBC ($r = 0.70$, $p = 1.9 \times 10^{-5}$). Fitting a linear regression model between MBC
392 and the rate of resistance change (i.e., the polynomial regression coefficient) results in a
393 coefficient of determination of $R^2 = 0.50$, slope of 20.54, and 95% CI [12.10, 29.06] (Figure 4).
394 We also observed a weaker negative correlation with the ratio GLC:NAG ($r = -0.40$, $p = 0.03$,
395 slope=-47.66, 95% CI [-92.75, -2.58]), which has been considered as an index for early chitin
396 decomposition processes [75]. A significant but weak correlation is also observed with SOC ($r =$
397 0.40 , $p = 0.03$, slope=52.51, 95% CI [6.59, 98.42]). We should note that these correlations are
398 not meant to serve as a calibration curve but rather indicate a strong pattern relating sensor
399 decomposition rate to associated measurable parameters. Two apparent visual outliers occurring
400 at higher MBC contents and having higher sensor slopes were examined in an outlier analysis,
401 where we determined their inclusion is appropriate after examining the sensor signals (see the
402 supplementary information for discussion, with Table S1 and Figures S8-S13). Removing these
403 signals from the analysis results in a weaker but still-significant correlation with MBC ($r = 0.48$,
404 $p = 0.03$, 95% CI [2.9×10^{-3} , 2.1×10^{-2}]).



405

406 **Figure 4.** A single decomposition window analysis showed a strong correlation between
407 measured plot-wise MBC values and sensor slopes. 95% CI shown in grey.

408 To test the impact of decomposition window selection on these results, a sensitivity analysis was
409 carried out by modifying window start and end dates and re-calculating correlations with MBC.
410 Four tests were carried out, expanding and contracting the decomposition window by 40% and
411 160% respectively, and moving the window 3 days left or 3 days right. All tests resulted in
412 statistically significant but lower correlation coefficients compared to the baseline test
413 (Supplementary Table S5).

414 *3.2.2 Analysis 2: Sensor-specific decomposition windows in two phases*

415 Considering two sensor-specific decomposition windows determined by changepoint analysis,
416 Phase 1 and Phase 2 slopes positively correlated to MBC ($r = 0.52$, $p = 0.003$, and $r = 0.526$, $p =$
417 0.0041 respectively). Weaker, yet still-significant correlations were found with SOC ($r = 0.37$, $p =$
418 0.043 , and $r = 0.424$, $p = 0.0222$ respectively). This suggests that there is utility to both
419 Analysis 1 and Analysis 2, with useful biological information extractable from the fleet as a
420 whole or from individual sensors, even at this early stage of sensor development.

421 *3.2.3 Analysis 3: Sensor-specific changepoint analysis*

422 This approach found correlations between the number of significant changepoints in the time
423 series data and laboratory measurements within plots. Statistically significant correlations were
424 found with a number of measurements (SOC $r = 0.53$, $p = 0.001$; PHO $r = 0.46$, $p = 0.006$; MBC
425 $r = 0.37$, $p = 0.033$, GLC $r = 0.36$, $p = 0.038$). It is worth noting that in the sites with higher
426 numbers of detected change points, we see a high number of detectable events over a relatively
427 short deployment period, suggesting that useful information can be gleaned by monitoring at this
428 relatively high frequency. It is also interesting that the more static carbon-related measurement,
429 SOC, correlates more strongly with the sensor signal in this approach than MBC does.

430 All of the data analysis approaches described here resulted in statistically significant correlations
431 with MBC and SOC, indicating a robust correlation to these soil properties. All statistically
432 significant results ($p < 0.05$) are shown below (Table 3). Results from fitting the linear regression
433 models to the laboratory measurements that have a significant correlation with the derived
434 metrics from Analysis 2 and Analysis 3 are presented in the supplemental Table S2.

435 Table 3: Decomposition sensor signal correlations to laboratory measurements (Pearson
436 correlation coefficient), all significant at $p < 0.05$. n.s. indicates no statistically significant
437 correlation was detected.

Soil health parameter

Method	MBC	GLC	NAG	PHO	GLC:NAG	SOC
Analysis 1	0.70	n.s.	n.s.	n.s.	-0.40	0.40
Analysis 2, Phase 1	0.52	n.s.	n.s.	n.s.	n.s.	0.37
Analysis 2, Phase 2	0.52	n.s.	n.s.	n.s.	n.s.	0.42
Analysis 3	0.37	0.36	n.s.	0.46	n.s.	0.53

438

439 3.2.3 Interference Experiments

440 The interference experiments showed repeatable and reversible responses of measured resistance
441 as a function of soil moisture, temperature, and conductivity. Varying temperature between 5.4
442 and 23.5 °C resulted in normalized sensor resistances from 1.06 to 0.86, showing an inverse
443 relationship with temperature. Varying soil moisture between 18.9% and 46.4% VWC resulted in
444 normalized resistances between 0.83 and 1.44, and varying soil conductivity between 437 and
445 1120 $\mu\text{S}/\text{cm}$ showed an inverse relationship with normalized resistances between 0.6 and 1.0.
446 Timeseries plots showing normalized resistance changes across these conditions are shown in
447 Supplementary Figure S17.

448 These results suggest that while field conditions do impact the resistivity of the substrate and
449 therefore logged resistance readings, these impacts are predictable, temporary and reversible.
450 Moreover, it is important to note that since all sensors in this experiment were co-located in the
451 same field, the impacts of rain and diurnal temperature variations are shared across the fleet,
452 constituting a background signal shared by all sensors.

453 3.3. Potential Application and Implications for Environmental Monitoring

454 The sensor described here shows initial promise in enabling scalable, in-situ data collection that
455 relates to widely used soil biological properties related to soil health. Low-cost printed microbial
456 sensors could support efforts to track and verify the rehabilitation of degraded land and
457 contribute to food security-related environmental monitoring. We have shown here that several
458 statistical approaches suggest a robust relationship between the sensor signal and measurements
459 of microbial biomass carbon and soil organic carbon, important indicators of soil health. The
460 other analysis approaches described here found weaker but still significant correlations with
461 other important field measurements, including GLC, PHO, and the GLC:NAG ratio. With
462 improvements to the fabrication and interrogation of these decomposition sensors, scalable, low-
463 cost deployments could help overcome current limitations in soil biological health monitoring
464 programs.

465 Prominently, all three analysis approaches found significant correlations between the sensor
466 signal and measured MBC and SOC values in instrumented plots. Prior studies have shown a
467 positive correlation between MBC and organic matter mineralization [76,77], and have, in fact,
468 posited it as a more useful indicator when compared with other forms of SOC, including
469 particulate organic carbon (POC) and mineral associated organic carbon (MAOC) [78]. MBC is
470 also often used as a biological indicator of soil health, showing promise as an early indicator of
471 ecological change following land use change and changes in agricultural practices [79–82]. A
472 low-cost and easily distributable solution for MBC-proxy tracking could offer a new high-
473 spatiotemporal resolution window into these dynamics.

474 A potential application for this sensing approach is to continuously monitor proxy signals for the
475 soil microbiome's metabolism and activity immediately following environmental perturbations.
476 This could yield useful insights into the resilience of the microbial community in the face of
477 shocks including droughts or agricultural practices like pest fumigation. A more mature
478 instantiation of these decomposition sensors could help to determine whether critical nutrient
479 cycling capacity is impacted by such events and help to characterize the resilience of the soil
480 microbiome by monitoring changes in microbial activity over time.

481 **3.4. Strengths and Limitations**

482 This sensing modality offers new opportunities to monitor decomposition activity in real time
483 and at low cost. Significant opportunities might lie in the exploration of other conductor
484 formulations, applied to a similar deployment platform but targeting other decomposition
485 pathways by selecting alternate binders. Some applicable binder materials might include lignin,
486 cellulose, or location-specific plant litter.

487 Another valuable aspect of the sensor response is that the signal should be related only to living
488 microbes, avoiding issues associated with relic DNA and enhancing the sensor's specificity. This
489 might be especially important for environments where the soil microbiome changes seasonally.

490 A primary challenge in interpreting this sensor data and making the results useful is the
491 stochastic response of individual sensors, both initially on installation and as decomposition rates
492 increase and sensors begin to fail. Upon insertion, the resistor can be damaged, rendering the
493 sensor useless; even with great care taken during installation, one sensor's initial resistance in
494 this study indicated that physical damage had immediately occurred. Furthermore, if sensor
495 failure is rapid, the useful life of the sensor can be meaningfully reduced. In this experiment,
496 using sensors with a single loop of substrate, the rate of sensor failure was high: 13 of 44 total
497 installed sensors (29.5%) were removed from the final analysis due to rapid failure, high initial
498 resistance, or a non-response signal. Time to failure was not found to have a statistically
499 significant correlation to measured soil parameters. To address these issues, ongoing work is
500 examining approaches to control the degradation process through material and hardware
501 modifications to improve reliability and reduce sensor-to-sensor variability. One approach may

502 be to combine multiple sensing surfaces, decreasing the impact of any individual sensor trace
503 failure.

504 Another challenge lies in the time-integrated nature of the readings derived in this research.
505 While we have stressed the intensive nature of traditional laboratory measurements in yielding
506 actionable data for soil health, one limitation of this technology is that a usable reading requires
507 ongoing monitoring of the sensor signal. Future work must quantify the deployment time
508 required for a sensor which uses this modality to produce readings, which may be a function of
509 biological and physical characteristics at deployment sites. Tied to this, design decisions related
510 to deployment platforms need to be considered. Local logging systems like the one used here can
511 function continuously with extremely low power consumption, but a sensor network that enables
512 more active management decisions would likely need to incorporate telemetry solutions which
513 bring with them significant logistical challenges and higher deployment costs and complexity.

514 This experiment deployed sensors across plots at one outdoor site and across a single season.
515 Therefore, the extensibility of these results is not yet clear. Experiments across various soil types
516 and weather conditions are necessary in the future to establish the contexts in which these
517 sensors can serve as a proxy for biological soil health. Additionally, no co-located in-situ sensors
518 were deployed in this experiment, limiting our ability to examine sources of interference in the
519 sensor signal. These novel sensors are directly measuring substrate decomposition, rather than
520 the upstream drivers, which include both microbial processes and abiotic drivers like changes in
521 soil moisture and temperature. Ultimately, we are primarily interested in measuring
522 decomposition rates, which are driven by complex soil dynamics including physical and
523 chemical processes. These drivers must be examined in future research to decouple biotic and
524 abiotic influence. While we have started to characterize immediate environmental impacts on
525 sensor signals here, observing significant but reversible resistance changes due to changes in soil
526 moisture, temperature and conductivity, future work should include co-located soil temperature,
527 moisture, pH, and respiration sensors.

528 In this work, we evaluate sensor signals which are the result of changes to a biodegradable
529 substrate. These changes are downstream of primary drivers including microbial community
530 composition and dynamic soil conditions like moisture, pH and temperature. Significant future
531 work must be undertaken to characterize the sensor's response to other abiotic drivers, and to
532 establish what microbial communities are responsible for the sensor signal. This work should
533 include genetic analysis and expanded testing, including quantification of sensor signals in a
534 wider range of live and sterilized soils and analysis of the impacts of abiotic drivers.

535 **4. Conclusion**

536 This report describes the first field deployment of a novel soil sensor designed to determine
537 microbial decomposition activity through a unique transduction mechanism based on a soil
538 degradable resistor. These low-cost sensors, manufactured from readily available materials using

539 printing approaches and addressable by simple electronics, are a step towards spatially dense
540 data collection of parameters related to biological soil health. This study analyzed the signal
541 from 31 sensors over 50 days at an experimental field site with varying soil properties. Three
542 approaches for extracting data from the sensor signal were evaluated, with the principal finding
543 that all analyses demonstrated a robust correlation to microbial biomass carbon and soil organic
544 carbon.

545 Future work will focus on improving manufacturing quality control and decreasing sensor failure
546 rates by mitigating the impacts of individual decomposition trace failure. Multiple traces will be
547 printed on each sensing surface and their signals multiplexed or smoothed. Controlled
548 interference experiments with co-located soil sensors are needed to help to characterize biotic
549 and abiotic drivers of the sensor signal, and genetic analysis of instrumented soil samples can
550 identify what microbes are responsible for trace decomposition. Multiple soils and seasons must
551 be instrumented to establish generalizability of this sensing modality, along with larger-scale
552 deployments across diverse sites. Logger hardware development will focus on field telemetry,
553 enabling long-distance data collection via radio or satellite signal.

554 This experiment is a first step towards validating a new sensing modality which shows promise
555 as a proxy for soil biological processes. The results described here suggest potential future
556 applications for these in-situ transient decomposition sensors to help characterize soil health
557 trajectories at high resolution and low cost, aligning with the need for larger spatial and temporal
558 scales of soil microbiome monitoring.

559 **Data Availability Statement**

560 Raw datalogger datasets, a plot lookup table, and soil property measurement data are hosted on
561 the Open Science Framework. These resources are openly available at the following DOI:
562 <https://doi.org/10.17605/OSF.IO/K98Q4>

563 **Acknowledgements**

564 This work was funded by the US Department of Agriculture, National Institute for Food and
565 Agriculture, (USDA NIFA) award: 2019–05291, and the UK Natural Environment Research
566 Council (NERC) award: NE/T012307/1.

567

568 **References**

- 569 [1] Robinson DA, Fraser I, Dominati EJ, Davíðsdóttir B, Jónsson JOG, Jones L, et al. On the
570 value of soil resources in the context of natural capital and ecosystem service delivery. *Soil Sci*
571 *Soc Am J* 2014;78:685–700.
- 572 [2] Wiesmeier M, Urbanski L, Hobbey E, Lang B, von Lützow M, Marin-Spiotta E, et al. Soil
573 organic carbon storage as a key function of soils - A review of drivers and indicators at various
574 scales. *Geoderma* 2019;333:149–62.
- 575 [3] Veum KS, Sudduth KA, Kremer RJ, Kitchen NR. Sensor data fusion for soil health
576 assessment. *Geoderma* 2017;305:53–61.
- 577 [4] Arias M. Soil health: new challenge microbiologists chemists. *International Microbiology*
578 2005;8:13–21.
- 579 [5] Lehmann J, Bossio DA, Kögel-Knabner I, Rillig MC. The concept and future prospects
580 of soil health. *Nat Rev Earth Environ* 2020;1:544–53.
- 581 [6] Powlson DS. Soil health - useful terminology communication meaningless concept?
582 both? *Frontiers Agricultural Science Engineering* 2020;7:246–50.
- 583 [7] Steinberger Y, Stein A, Dorman M, Svoray T, Doniger T, Rinot O, et al. A sensitive soil
584 biological indicator to changes in land-use in regions with Mediterranean climate. *Sci Rep*
585 2022;12. <https://doi.org/10.1038/s41598-022-26240-9>.
- 586 [8] Griffiths BS, Faber J, Bloem J. Applying soil health indicators to encourage sustainable
587 soil use: The transition from scientific study to practical application. *Sustainability*
588 2018;10:3021.
- 589 [9] Doran JW, Zeiss MR. Soil health and sustainability: managing the biotic component of
590 soil quality. *Appl Soil Ecol* 2000;15:3–11.
- 591 [10] Fan Y, Wang X, Funk T, Rashid I, Herman B, Bompoti N, et al. A critical review for
592 real-time continuous soil monitoring: Advantages, challenges, and perspectives. *Environ Sci*
593 *Technol* 2022;56:13546–64.
- 594 [11] Fierer N. Embracing the unknown: disentangling the complexities of the soil
595 microbiome. *Nat Rev Microbiol* 2017;15:579–90.
- 596 [12] Robertson GP. Standard soil methods for long-term ecological research. London,
597 England: Oxford University Press; 1999.

- 598 [13] Hanselman TA, Graetz DA, Obreza TA. A comparison of in situ methods for measuring
599 net nitrogen mineralization rates of organic soil amendments. *J Environ Qual* 2004;33:1098–105.
- 600 [14] Harmon M, Nadelhoffer K, Blair J, Robertson G, Coleman D, Bledsoe C, et al.
601 Measuring decomposition, nutrient turnover, and stores in plant litter 1999:202–40.
- 602 [15] Keuskamp JA, Dingemans BJJ, Lehtinen T, Sarneel JM, Hefting MM. Tea Bag Index: a
603 novel approach to collect uniform decomposition data across ecosystems. *Methods Ecol Evol*
604 2013;4:1070–5.
- 605 [16] Pumpanen J, Longdoz B, L. Kutsch W. Field measurements of soil respiration: principles
606 and constraints, potentials and limitations of different methods. In: Kutsch WL, Bahn M,
607 Heinemeyer A, editors. *Soil Carbon Dynamics*, Cambridge: Cambridge University Press; 2010,
608 p. 16–33.
- 609 [17] Clément CC, Burton DL, Laurence L, Fehr PA, Congreves KA, Dessureault-Rompré J.
610 Nitrogen mineralization in Canadian agricultural soils: a review of methods for quantifying soil
611 nitrogen mineralization potential and estimating growing season nitrogen mineralization. *Can J*
612 *Soil Sci* 2025;105:1–19.
- 613 [18] Vance ED, Brookes PC, Jenkinson DS. An extraction method for measuring soil
614 microbial biomass C. *Soil Biol Biochem* 1987;19:703–7.
- 615 [19] Greenfield LM, Puissant J, Jones DL. Synthesis of methods used to assess soil protease
616 activity. *Soil Biol Biochem* 2021;158:108277.
- 617 [20] Zelles L. Fatty acid patterns of phospholipids and lipopolysaccharides in the
618 characterisation of microbial communities in soil: a review. *Biol Fertil Soils* 1999;29:111–29.
- 619 [21] Zwolinski MD. DNA sequencing: Strategies for soil microbiology. *Soil Sci Soc Am J*
620 2007;71:592–600.
- 621 [22] Pan H, Wattiez R, Gillan D. Soil metaproteomics for microbial community profiling:
622 Methodologies and challenges. *Curr Microbiol* 2024;81:257.
- 623 [23] Tang J, Baldocchi DD, Qi Y, Xu L. Assessing soil CO₂ efflux using continuous
624 measurements of CO₂ profiles in soils with small solid-state sensors. *Agric For Meteorol*
625 2003;118:207–20.
- 626 [24] Atreya M, Desousa S, Kauzya J-B, Williams E, Hayes A, Dikshit K, et al. A transient
627 printed soil decomposition sensor based on a biopolymer composite conductor. *Adv Sci (Weinh)*
628 2023;10:e2205785.

- 629 [25] Dubey A, Malla MA, Khan F, Chowdhary K, Yadav S, Kumar A, et al. Soil microbiome:
630 a key player for conservation of soil health under changing climate. *Biodivers Conserv*
631 2019;28:2405–29.
- 632 [26] Orwin KH, Stevenson BA, Smaill SJ, Kirschbaum MUF, Dickie IA, Clothier BE, et al.
633 Effects of climate change on the delivery of soil-mediated ecosystem services within the primary
634 sector in temperate ecosystems: a review and New Zealand case study. *Glob Chang Biol*
635 2015;21:2844–60.
- 636 [27] Delgado-Baquerizo M, Reich PB, Trivedi C, Eldridge DJ, Abades S, Alfaro FD, et al.
637 Multiple elements of soil biodiversity drive ecosystem functions across biomes. *Nat Ecol Evol*
638 2020;4:210–20.
- 639 [28] Bhattacharyya SS, Ros GH, Furtak K, Iqbal HMN, Parra-Saldivar R. Soil carbon
640 sequestration - An interplay between soil microbial community and soil organic matter
641 dynamics. *Sci Total Environ* 2022;815:152928.
- 642 [29] Sáez-Sandino T. The soil microbiome governs response microbial respiration warming
643 across globe. *Nature Climate Change* 2023;13:1382–7.
- 644 [30] Sokol NW, Slessarev E, Marschmann GL, Nicolas A, Blazewicz SJ, Brodie EL, et al.
645 Life and death in the soil microbiome: how ecological processes influence biogeochemistry. *Nat*
646 *Rev Microbiol* 2022;20:415–30.
- 647 [31] Brevik EC, Pereg L, Steffan JJ, Burgess LC. Soil ecosystem services and human health.
648 *Curr Opin Environ Sci Health* 2018;5:87–92.
- 649 [32] Herrick JE, Abrahamse T, Abhilash PC, Ali SH, Alvarez-Torres P, Barau S, et al. Land
650 Restoration Achieving Sustainable Development Goals: International Resource Panel Think
651 Piece. Think Piece International Resource Panel United Nations Environment Programme n.d.
- 652 [33] Kumar A, Kim H, Hancke GP. Environmental Monitoring Systems: A Review. *IEEE*
653 *Sens J* 2013;13:1329–39.
- 654 [34] Xu X, Thornton PE, Post WM. A global analysis soil microbial biomass carbon, nitrogen
655 phosphorus terrestrial ecosystems. *Global Ecology Biogeography* 2013;22:737–49.
- 656 [35] Shirahama Y, Shigeta R, Kawahara Y, Asami T, Kojima Y, Nishioka K. Implementation
657 of wide range soil moisture profile probe by coplanar plate capacitor on film substrate. 2015
658 *IEEE SENSORS, IEEE*; 2015. <https://doi.org/10.1109/icsens.2015.7370633>.

- 659 [36] Sui Y, Atreya M, Dahal S, Gopalakrishnan A, Khosla R, Whiting GL. Controlled
660 Biodegradation of an Additively Fabricated Capacitive Soil Moisture Sensor. *ACS Sustain Chem*
661 *Eng* 2021;21:52.
- 662 [37] Atreya M, Dikshit K, Marinick G, Nielson J, Bruns C, Whiting GL. Poly(lactic acid)-
663 based ink for biodegradable printed electronics with conductivity enhanced through solvent
664 aging. *ACS Appl Mater Interfaces* 2020;12:23494–501.
- 665 [38] Ait-Mammar W, Zrig S, Bridonneau N, Noël V, Stavrinidou E, Piro B, et al. All-Inkjet-
666 Printed Humidity Sensors for the Detection of Relative Humidity in Air and Soil— Towards the
667 Direct Fabrication on Plant Leaves. *MRS Advances* 4 2020;5:965–73.
668 <https://doi.org/10.1557/ADV.2020.86/METRICS>.
- 669 [39] Singh M, Patkar RS, Vinchurkar M, Baghini MS. Cost effective soil pH sensor using
670 carbon-based screen-printed electrodes. *IEEE Sens J* 2020;20:47–54.
- 671 [40] Aliyana AK, Ganguly P, Beniwal A, Kumar SKN, Dahiya R. Disposable pH sensor on
672 paper using screen-printed graphene-carbon ink modified zinc oxide nanoparticles. *IEEE Sens J*
673 2022;22:21049–56.
- 674 [41] Galdino FE, Smith JP, Kwamou SI, Kampouris DK, Iniesta J, Smith GC, et al. Graphite
675 screen-printed electrodes applied for the accurate and reagentless sensing of pH. *Anal Chem*
676 2015;87:11666–72.
- 677 [42] Artigas J, Jimenez C, Lemos SG, Nogueira ARA, Torre-Neto A, Alonso J. Development
678 of a screen-printed thick-film nitrate sensor based on a graphite-epoxy composite for agricultural
679 applications. *Sens Actuators B Chem* 2003;88:337–44.
- 680 [43] Garland NT, McLamore ES, Cavallaro ND, Mendivelso-Perez D, Smith EA, Jing D, et
681 al. Flexible laser-induced graphene for nitrogen sensing in soil. *ACS Appl Mater Interfaces*
682 2018;10:39124–33.
- 683 [44] Baumbauer CL, Goodrich PJ, Payne ME, Anthony T, Beckstoffer C, Toor A, et al.
684 Printed potentiometric nitrate sensors for use in soil. *Sensors (Basel)* 2022;22:4095.
- 685 [45] Ali MA, Wang X, Chen Y, Jiao Y, Mahal NK, Moru S, et al. Continuous monitoring of
686 soil nitrate using a miniature sensor with poly(3-octyl-thiophene) and molybdenum disulfide
687 nanocomposite. *ACS Appl Mater Interfaces* 2019;11:29195–206.
- 688 [46] Cranny A, Harris NR, Nie M, Wharton JA, Wood RJK, Stokes KR. Screen-printed
689 potentiometric Ag/AgCl chloride sensors: Lifetime performance and their use in soil salt
690 measurements. *Sens Actuators A Phys* 2011;169:288–94.

- 691 [47] Cranny A, Harris N, White N. Screen Printed Potentiometric Chloride Sensors. *Procedia*
692 *Eng* 2014;87:220–3.
- 693 [48] Meereboer KW, Misra M, Mohanty AK. Review of recent advances in the
694 biodegradability of polyhydroxyalkanoate (PHA) bioplastics and their composites. *Green Chem*
695 2020;22:5519–58.
- 696 [49] Smith RS, Shiel RS, Bardgett RD, Millward D, Corkhill P, Evans P, et al. Long-term
697 change in vegetation and soil microbial communities during the phased restoration of traditional
698 meadow grassland. *J Appl Ecol* 4 2008;45:670–9.
- 699 [50] Smith RS, Shiel RS, Millward D, Corkhill P. The interactive effects of management on
700 the productivity and plant community structure of an upland meadow: an 8-year field trial. *J*
701 *Appl Ecol* 2000;37:1029–43.
- 702 [51] De Long JR, Jackson BG, Wilkinson A, Pritchard WJ, Oakley S, Mason KE, et al.
703 Relationships between plant traits, soil properties and carbon fluxes differ between monocultures
704 and mixed communities in temperate grassland. *J Ecol* 2019;107:1704–19.
- 705 [52] Liu S, Ward SE, Wilby A, Manning P, Gong M, Davies J, et al. Multiple targeted
706 grassland restoration interventions enhance ecosystem service multifunctionality. *Nat Commun*
707 2025;16:3971.
- 708 [53] Future of farming in England. Gov.uk 2023.
709 <https://www.gov.uk/government/collections/future-of-farming-in-england> (accessed May 19,
710 2024).
- 711 [54] Bilton AR. Does biodiversity restoration enhance the capacity of ecosystem functions to
712 buffer climate extremes? PhD. The University of Manchester, 2024.
- 713 [55] Cole AJ, Griffiths RI, Ward SE, Whitaker J, Ostle NJ, Bardgett RD. Grassland
714 biodiversity restoration increases resistance of carbon fluxes to drought. *J Appl Ecol*
715 2019;56:1806–16.
- 716 [56] De Deyn GB, Quirk H, Oakley S, Ostle N, Bardgett RD. Rapid transfer of photosynthetic
717 carbon through the plant-soil system in differently managed species-rich grasslands.
718 *Biogeosciences* 2011;8:1131–9.
- 719 [57] Smith RS, Shiel RS, Bardgett RD, Millward D, Corkhill P, Rolph G, et al. Soil microbial
720 community, fertility, vegetation and diversity as targets in the restoration management of a
721 meadow grassland. *J Appl Ecol* 2003;40:51–64.

- 722 [58] Bardgett RD, McAlister E. The measurement of soil fungal:bacterial biomass ratios as an
723 indicator of ecosystem self-regulation in temperate meadow grasslands. *Biol Fertil Soils*
724 1999;29:282–90.
- 725 [59] Jackson CR, Tyler HL, Millar JJ. Determination of microbial extracellular enzyme
726 activity in waters, soils, and sediments using high throughput microplate assays. *J Vis Exp* 2013.
727 <https://doi.org/10.3791/50399>.
- 728 [60] Brookes PC, Landman A, Pruden G, Jenkinson DS. Chloroform fumigation and the
729 release of soil nitrogen: A rapid direct extraction method to measure microbial biomass nitrogen
730 in soil. *Soil Biol Biochem* 1985;17:837–42.
- 731 [61] Killick R, Fearnhead P, Eckley IA. Optimal detection of changepoints with a linear
732 computational cost. *J Am Stat Assoc* 2012;107:1590–8.
- 733 [62] Smith P. How long before a change in soil organic carbon can be detected? *Glob Chang*
734 *Biol* 2004;10:1878–83.
- 735 [63] Killick R, Beaulieu C, Taylor S, Hullait H. Detection of structural changes in climate and
736 environment time series 2025.
- 737 [64] Killick R, Eckley IA. changepoint: AnRPackage for Changepoint Analysis. *J Stat Softw*
738 2014;58. <https://doi.org/10.18637/jss.v058.i03>.
- 739 [65] Zeileis A, Hothorn T. lmtest: Diagnostic Checking in Regression Relationships. *R News*
740 2002;2:7–10.
- 741 [66] Met Office. MIDAS: UK Hourly Weather Observation Data. NCAS British Atmospheric
742 Data Centre 2006.
- 743 [67] Alkorta I, Aizpurua A, Riga P, Albizu I, Amézaga I, Garbisu C. Soil enzyme activities as
744 biological indicators of soil health. *Rev Environ Health* 2003;18:65–73.
- 745 [68] Zhou L, Ding M. Soil microbial characteristics bioindicators soil health. *Biodiversity*
746 *Science* 2007;15.
- 747 [69] Sparling GP. Soil microbial biomass, activity and nutrient cycling as indicators of soil
748 health. In: Pankhurst C, Doube BM, Gupta VVSR, editors., *Manaaki Whenua - Landcare*
749 *Research*; 1997, p. 97–119.
- 750 [70] McGonigle T, Turner W. Grasslands and croplands have different microbial biomass
751 carbon levels per unit of soil organic carbon. *Agriculture* 2017;7:57.

- 752 [71] Ashraf MN, Hu C, Wu L, Duan Y, Zhang W, Aziz T, et al. Soil and microbial biomass
753 stoichiometry regulate soil organic carbon and nitrogen mineralization in rice-wheat rotation
754 subjected to long-term fertilization. *J Soils Sediments* 2020;20:3103–13.
- 755 [72] Nannipieri P, Ascher J, Ceccherini MT, Landi L, Pietramellara G, Renella G. Microbial
756 diversity and soil functions. *Eur J Soil Sci* 2017;68:12–26.
- 757 [73] Wardle DA. Controls of temporal variability of the soil microbial biomass: A global-
758 scale synthesis. *Soil Biol Biochem* 1998;30:1627–37.
- 759 [74] Karaca A, Cetin SC, Turgay OC, Kizilkaya R. Soil enzymes as indication of soil quality.
760 *Soil Biology, Berlin, Heidelberg: Springer Berlin Heidelberg*; 2010, p. 119–48.
- 761 [75] Mori T, Aoyagi R, Kitayama K, Mo J. Does the ratio of β -1,4-glucosidase to β -1,4-N-
762 acetylglucosaminidase indicate the relative resource allocation of soil microbes to C and N
763 acquisition? *Soil Biol Biochem* 2021;160:108363.
- 764 [76] Shu X, Hu Y, Liu W, Xia L, Zhang Y, Zhou W, et al. Linking between soil properties,
765 bacterial communities, enzyme activities, and soil organic carbon mineralization under
766 ecological restoration in an alpine degraded grassland. *Front Microbiol* 2023;14:1131836.
- 767 [77] Wu H, Cai A, Xing T, Huai S, Zhu P, Xu M, et al. Fertilization enhances mineralization
768 of soil carbon and nitrogen pools by regulating the bacterial community and biomass. *J Soils*
769 *Sediments* 2021;21:1633–43.
- 770 [78] Dong L, Fan J, Li J, Zhang Y, Liu Y, Wu J, et al. Forests have a higher soil C
771 sequestration benefit due to lower C mineralization efficiency: Evidence from the central loess
772 plateau case. *Agric Ecosyst Environ* 2022;339:108144.
- 773 [79] Zhang Q, Miao F, Wang Z, Shen Y, Wang G. Effects of long-term fertilization
774 management practices on soil microbial biomass in China’s cropland: A meta-analysis. *Agron J*
775 2017;109:1183–95.
- 776 [80] Vallejo VE, Roldan F, Dick RP. Soil enzymatic activities and microbial biomass in an
777 integrated agroforestry chronosequence compared to monoculture and a native forest of
778 Colombia. *Biol Fertil Soils* 2010;46:577–87.
- 779 [81] Tripathi S, Chakraborty A, Chakrabarti K, Bandyopadhyay BK. Enzyme activities and
780 microbial biomass in coastal soils of India. *Soil Biol Biochem* 11 2007;39:2840–8.
- 781 [82] Treseder KK. Nitrogen additions and microbial biomass: a meta-analysis of ecosystem
782 studies. *Ecol Lett* 2008;11:1111–20.